Supplementary Information

Organometallic Molecular Wires as Versatile Modules for Energy-Level Alignment of the Metal-Molecule-Metal Junction

Kaho Sugimoto,[a] Yuya Tanaka,*[a] Shintaro Fujii,[b] Tomofumi Tada,*[c]
Manabu Kiguchi*[b] Munetaka Akita,*[a]

[a] *Chemical Resources Laboratory, Tokyo Institute of Technology, R1-27, 4259 Nagatsuta Midori-ku, Yokohama 226-8503, Japan*
[b] *Department of Chemistry, Graduate School of Science and Engineering, Tokyo Institute of Technology, 2-12-1 W4-10, Ookayama, Meguro-ku, Tokyo 152-8551, Japan*
[c] *Materials Research Center for Element Strategy, Tokyo Institute of Technology, 4259 Nagatsuta-cho, Midori-ku, Yokohama, Kanagawa 226-8503, Japan*

E-mails: ytanaka@res.titech.ac.jp
makita@res.titech.ac.jp
kiguti@chem.titech.ac.jp
tada.t.ae@m.titech.ac.jp

Table of Contents

I. General

Materials

Reactions were performed under N_2 atmosphere using standard Schlenk tube technique. THF, CH_2Cl_2, diethyl ether, pentane were purified by Grubbs solvent system. Dry MeOH and Benzene were purchased from commercial sources and were used without further purification. Triethylamine was pre-dried by KOH and distilled over CaH. Other regent was used as received. Silica (Kanto chemical Co Inc. Silica Gel 60N) and alumina (Melck Alminium oxide 90 standardized) were used as received. 2-Bromo-5-trimethylsilylethynylthiophene,[S1] *cis*-$RuCl_2(dppe)_2$,[S2] 2,5-diethynylthiophene,[S3] $Ru[P(OMe)_3]_4Cl_2$,[S4] 4-ethynylpyridine,[S5] and $Ru(dmpe)_2(C{\equiv}CPy)_2$ (**3**) [S6] were synthesized according to the literature procedures.

Instruments

NMR spectra were recorded on Bruker biospin AVANCE Ⅲ 400 MHz spectrometers (^{1}H 400 MHz, ^{31}P 162 MHz) or Bruker biospin ASCEND-500 (^{13}C NMR 126 MHz). Solvent for NMR measurements were dried over molecular sieves, degassed, and stored under nitrogen. GC-MS and ESI-TOF-MS were performed on Shimadzu Corp. PARVUM2, and Bruker micrOTOF II, respectively. UV–Vis and IR spectra (KBr pellets) were obtained on a JASCO V670DS and FTIR 4200 spectrometer, respectively. Electrochemical measurements (CV and DPV) were made with a Hokutodenkou HZ-5000 analyzer (observed in CH_2Cl_2; [complex] = *ca.* 1×10^{-3} M; [NBu_4PF_6] = 0.1 M; working electrode: Pt, counter electrode: Pt, reference electrode: $Ag/AgNO_3$; scan rates were 100 mV/s (CV) and 25 mV/s (DPV)). After the measurement, ferrocene (Fc) was added to the mixture and the potentials were calibrated with respect to the Fc/Fc^+ redox couple. Recycled GPC was performed on JAI LC-9225NEXT. Elemental analyses were performed at the Center for Advanced Materials Analysis, Technical Department, Tokyo Institute of Technology.

II. STM-BJ measurement

The conductance measurements were performed using the scanning tunneling microscope (STM) break junction technique with electrochemical STM (Pico-SPM, Molecular Imaging Co.) and a Nano Scope IIIa controller (Digital Instruments Co.). Cells, beakers, ceramic tweezers, and Schlenk tubes used for STM-BJ measurements were cleaned by soaking with mixed acid prior to use. The STM-tips were made from an Au wire (0.30 mm diameter, *ca.* 1.3 cm long, and 99,99% purity, obtained from The Nilaco Corporation) coated with wax. The substrate of Au(111) was prepared from Au wires (0.90 mm diameter, *ca.* 5.0 cm long, and 99,99% purity, obtained from The Nilaco Corporation) by flame annealing and quenching after boiling with concentrated HCl solution. Solutions of molecular wires in tetraglyme (~1.0 mM) were used for the measurements. Conductance was measured during the breaking process under an applied bias of 100 mV.

Conductance histogram

Each break-junction measurement was repeated 100 times (1 set) and each set of the measurement was repeated 21 times (in total 2100 break-junction measurements for a individual experiment). Each histogram was made by each set of the measurements and the conductance of the molecules was determined on the basis of the reproducibility of the peaks observed at the histograms. The sets of the measurements were repeated at least 3 times. No preference or data selection was performed for the making histograms.

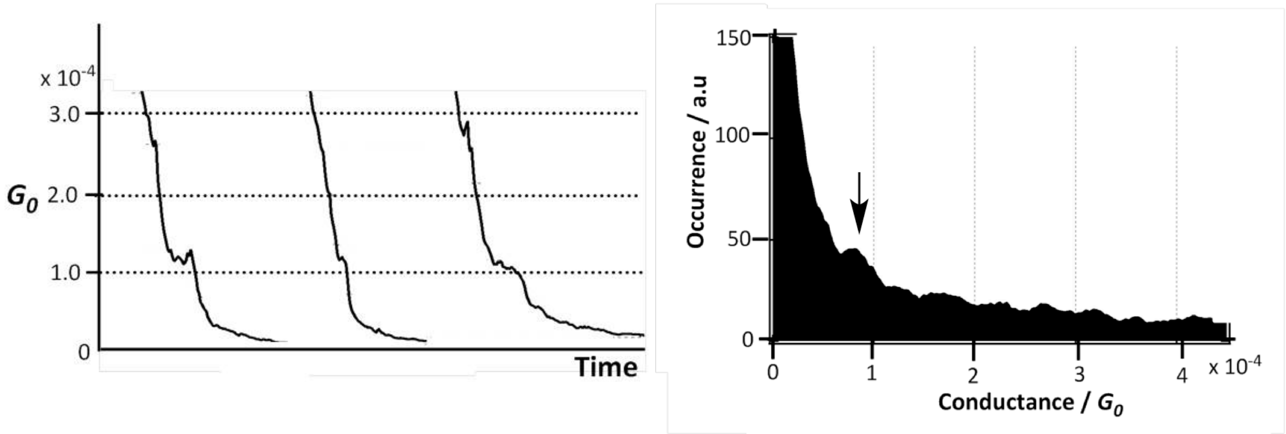

Figure S1. Typical conductance traces and histogram of **4**

Break junction process

The typical conductance traces obtained from STM-BJ measurements of **1-3** are shown in Figure S2. Immediately after the separation of the STM-tip and the gold substrates (A), where the conductance is 1 G_0, the conductance decreases with the increase of the stretch length. When a molecular junction forms (B), a step is observed at the position corresponding to the conductance of the molecule. The stretch length continues to increase, and then the molecular junction breaks (C).

The length of the conductance plateaus indicates the length of the contact period of molecular junctions (B), which does not always correspond to the molecular length. In particular, for the Ru wires **1-3**, the relatively bulky phosphine and phosphite ligands make the junction formation difficult and the contact periods become much shorter than those of molecular lengths of **1-3**.

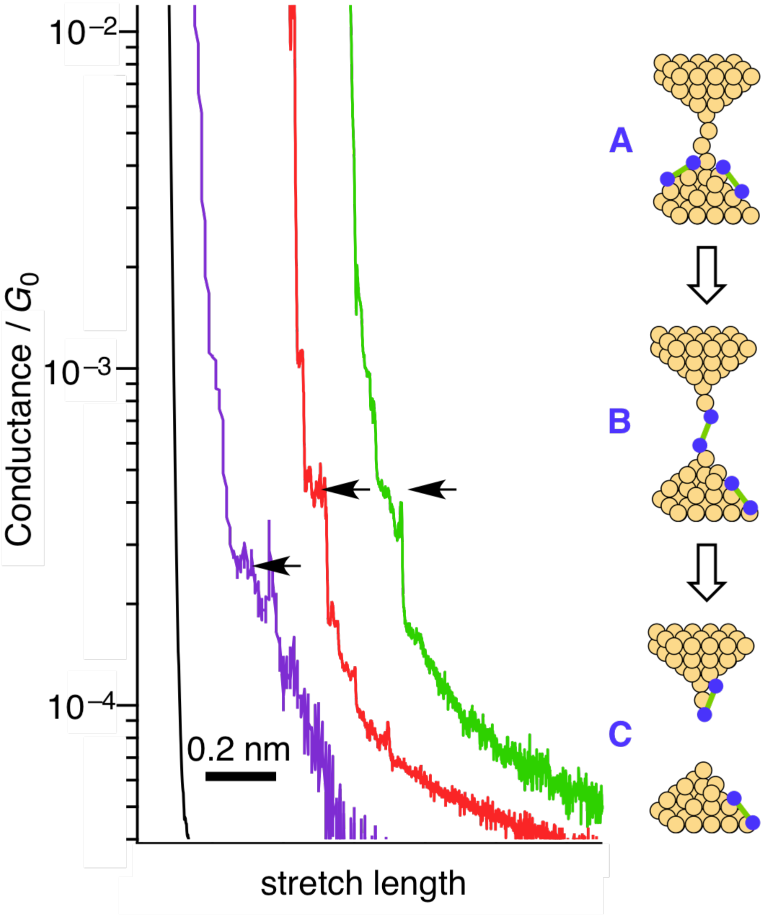

Figure S2. Typical conductance curves for blank (black), **1** (purple), **2** (red) and **3** (green) in tetraglyme solution. Allows indicate the position of the corresponding molecular junctions (B).

III. Synthesis

Synthesis of 1

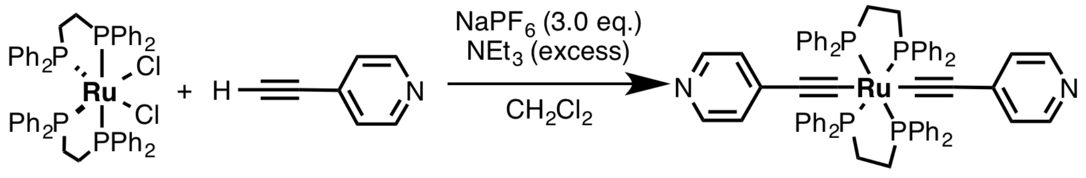

1

To a mixture of *cis*-$RuCl_2(dppe)_2$ (500 mg, 0.514 mmol) and $NaPF_6$ (259 mg, 1.54 mmol) in CH_2Cl_2 (30 mL) in the presence of molecular sieve 4A was added a triethylamine (1 mL) solution of 4-ethynylpyridine (159 mg, 1.54 mmol) and the resultant mixture was sttirred for 2 days at room temperature. The reaction mixture was evaporated *in vacuo* and the residue was washed with methanol and with pentane to give orange solid, which was dissolved in CH_2Cl_2 and precipitated with methanol to give **1** (163 mg, 0.147 mmol, 29%). The product is pure enough to be used for various measurements. The analytical pure sample and crystals for X-ray analysis were obtained by slow diffusion of methanol into CH_2Cl_2 solution of **1**.

^{1}H NMR (400 MHz, CD_2Cl_2, r.t.) : δ 8.25 (dd, 4H, , J_1 = 4.6 Hz, J_2 = 1.6, Py), 7.46-6.97 (m, 40H, dppe-Ph), 6.55(d, 4H, J_1 = 4.6 Hz, J_2 = 1.6, Py), 2.65 (*pseudo*-t, 8H, J = 8.0 Hz, dppe-CH_2). ^{31}P NMR (161 MHz, CD_2Cl_2, r.t.) : δ 52.7(s). ^{13}C NMR (126MHz, CD_2Cl_2): δ 148.9 (s, Py), 136 .8 (m, Ru-*C*≡), 134.4 (s, dppe-Ph), 129.3 (s, dppe-Ph), 127.6 (dppe-Ph), 125.0 (s, Py), 116.3 (s, C_q), 31.6 (*pseudo*-t, J = 12.6 Hz, dppe-CH_2). Some of the Quaternary carbon atoms could not be observed even in saturated CD_2Cl_2 solution. ESI-TOF MS (CH_2Cl_2 *m*/*z*): Calcd. for $C_{66}H_{57}N_2P_4Ru$: 1103.2548, Found. $[M+H]^+$: 1103.2528. IR (KBr): 2056 cm^{-1}(C≡C), Anal. Calcd. for $C_{66}H_{56}N_2P_4Ru \bullet CH_2Cl_2$: C, 67.79 ; H, 4.92, Found : C, 68.00 ; H, 4.83

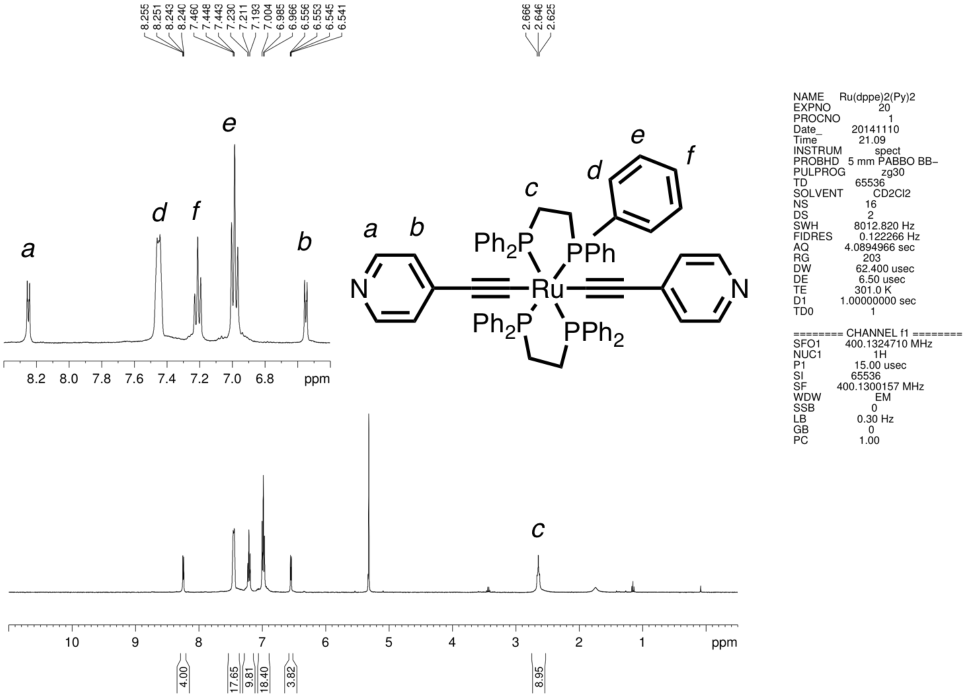

```
NAME     Ru(dppe)2(Py)2
EXPNO              20
PROCNO              1
Date_        20141110
Time            21.09
INSTRUM         spect
PROBHD   5 mm PABBO BB-
PULPROG          zg30
TD              65536
SOLVENT        CD2Cl2
NS                 16
DS                  2
SWH          8012.820 Hz
FIDRES       0.122266 Hz
AQ          4.0894966 sec
RG                203
DW             62.400 usec
DE               6.50 usec
TE              301.0 K
D1         1.00000000 sec
TD0                 1

======== CHANNEL f1 ========
SFO1       400.1324710 MHz
NUC1               1H
P1              15.00 usec
SI              65536
SF         400.1300157 MHz
WDW                EM
SSB                 0
LB               0.30 Hz
GB                  0
PC               1.00
```

Figure S3a. ^{1}H NMR spectrum of **1** (400 MHz, CD_2Cl_2, r.t.)

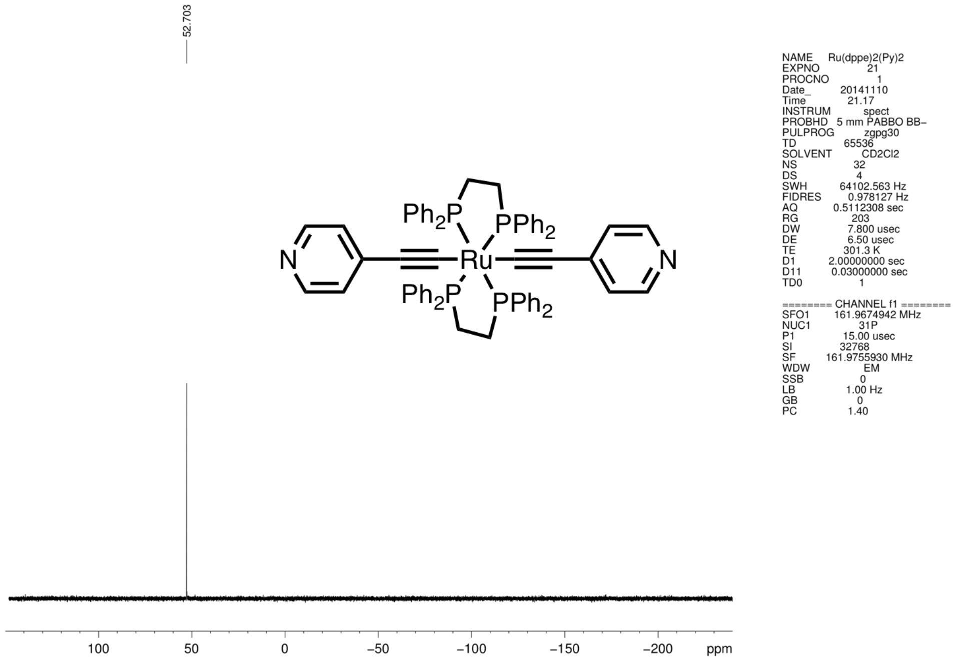

```
NAME     Ru(dppe)2(Py)2
EXPNO              21
PROCNO              1
Date_        20141110
Time            21.17
INSTRUM         spect
PROBHD   5 mm PABBO BB-
PULPROG        zgpg30
TD              65536
SOLVENT        CD2Cl2
NS                 32
DS                  4
SWH         64102.563 Hz
FIDRES       0.978127 Hz
AQ          0.5112308 sec
RG                203
DW              7.800 usec
DE               6.50 usec
TE              301.3 K
D1         2.00000000 sec
D11        0.03000000 sec
TD0                 1

======== CHANNEL f1 ========
SFO1       161.9674942 MHz
NUC1              31P
P1              15.00 usec
SI              32768
SF         161.9755930 MHz
WDW                EM
SSB                 0
LB               1.00 Hz
GB                  0
PC               1.40
```

Figure S3b. ^{31}P NMR spectrum of **1** (162 MHz, CD_2Cl_2, r.t.)

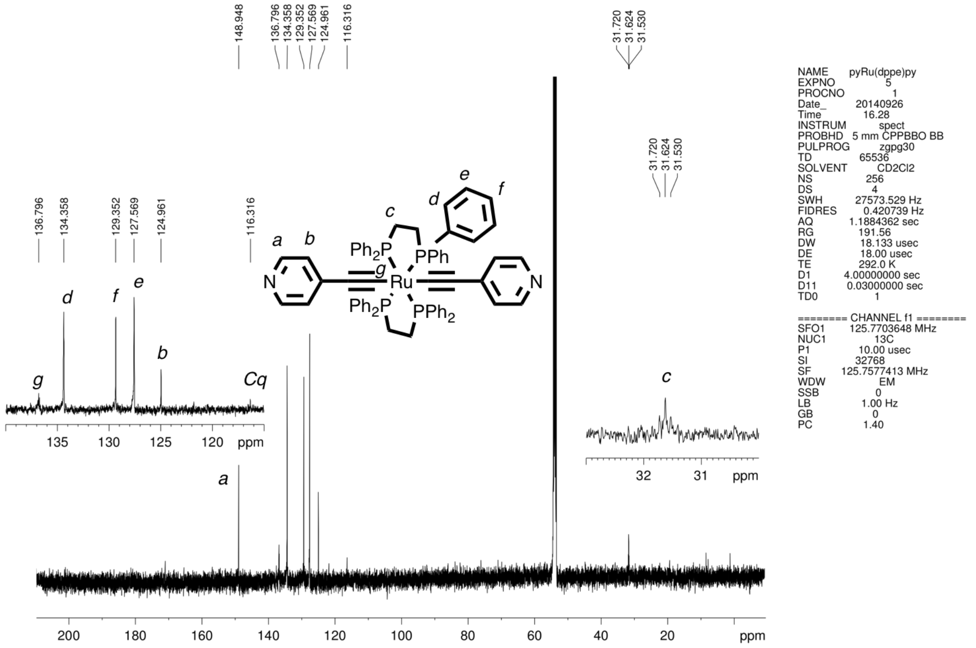

Figure S3c. ^{13}C NMR spectrum of **1** (126 MHz, CD_2Cl_2, r.t.)

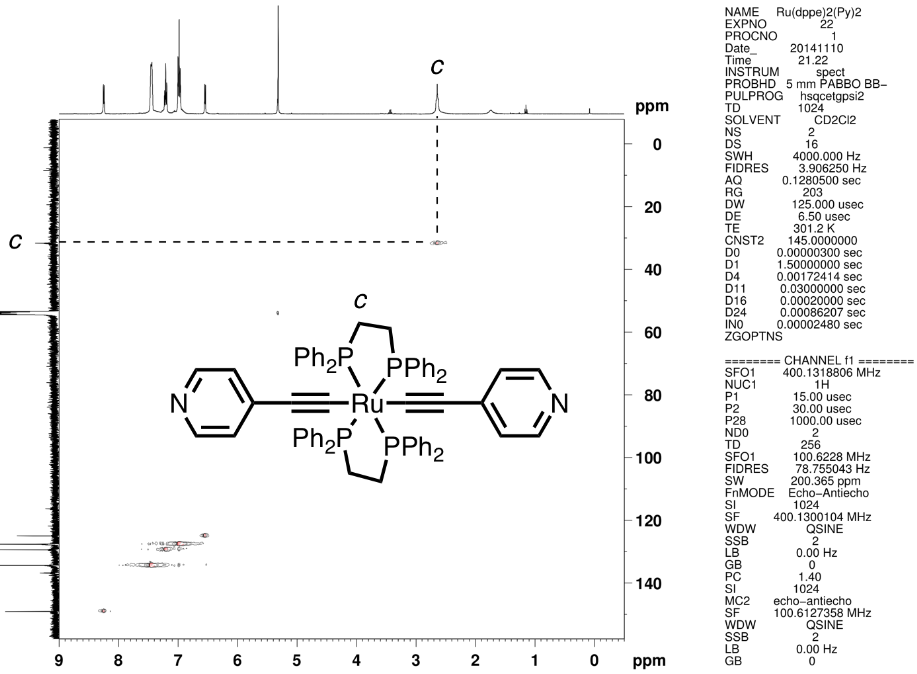

Figure S3d. ^{1}H-^{13}C HSQC NMR spectrum of **1** (400 MHz, CD_2Cl_2, r.t.)

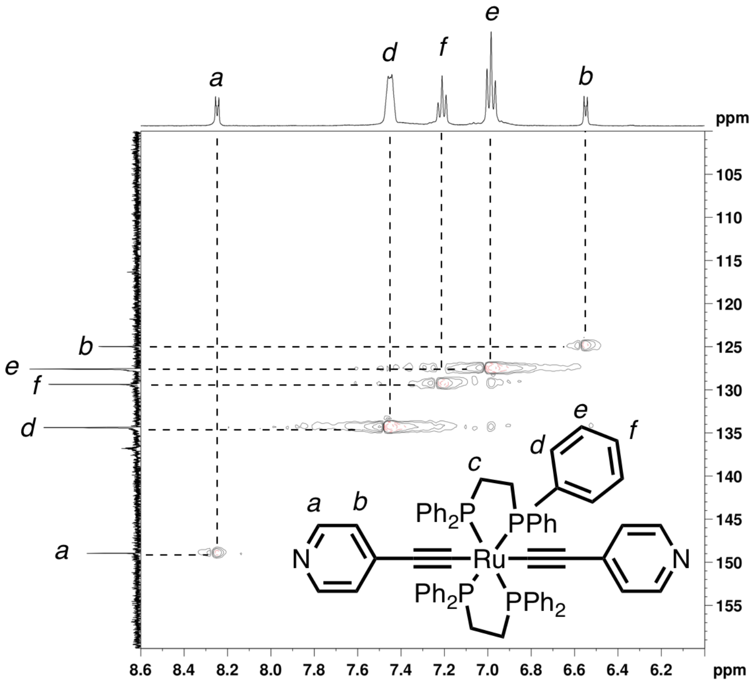

```
NAME     Ru(dppe)2(Py)2
EXPNO              22
PROCNO              1
Date_        20141110
Time            21.22
INSTRUM         spect
PROBHD   5 mm PABBO BB-
PULPROG   hsqcetgpsi2
TD              1024
SOLVENT        CD2Cl2
NS                 2
DS                16
SWH        4000.000 Hz
FIDRES     3.906250 Hz
AQ       0.1280500 sec
RG               203
DW       125.000 usec
DE          6.50 usec
TE           301.2 K
CNST2    145.0000000
D0      0.00000300 sec
D1      1.50000000 sec
D4      0.00172414 sec
D11     0.03000000 sec
D16     0.00020000 sec
D24     0.00086207 sec
IN0     0.00002480 sec
ZGOPTNS

======== CHANNEL f1 ========
SFO1     400.1318806 MHz
NUC1              1H
P1           15.00 usec
P2           30.00 usec
P28        1000.00 usec
ND0                2
TD               256
SFO1       100.6228 MHz
FIDRES     78.755043 Hz
SW         200.365 ppm
FnMODE    Echo-Antiecho
SI              1024
SF      400.1300104 MHz
WDW            QSINE
SSB                2
LB           0.00 Hz
GB                 0
PC              1.40
SI              1024
MC2     echo-antiecho
SF      100.6127358 MHz
WDW            QSINE
SSB                2
LB           0.00 Hz
GB                 0
```

Figure S3e. ^{1}H-^{13}C HSQC spectrum of **1** (400 MHz, $CD_2Cl_{2,}$ r.t.)

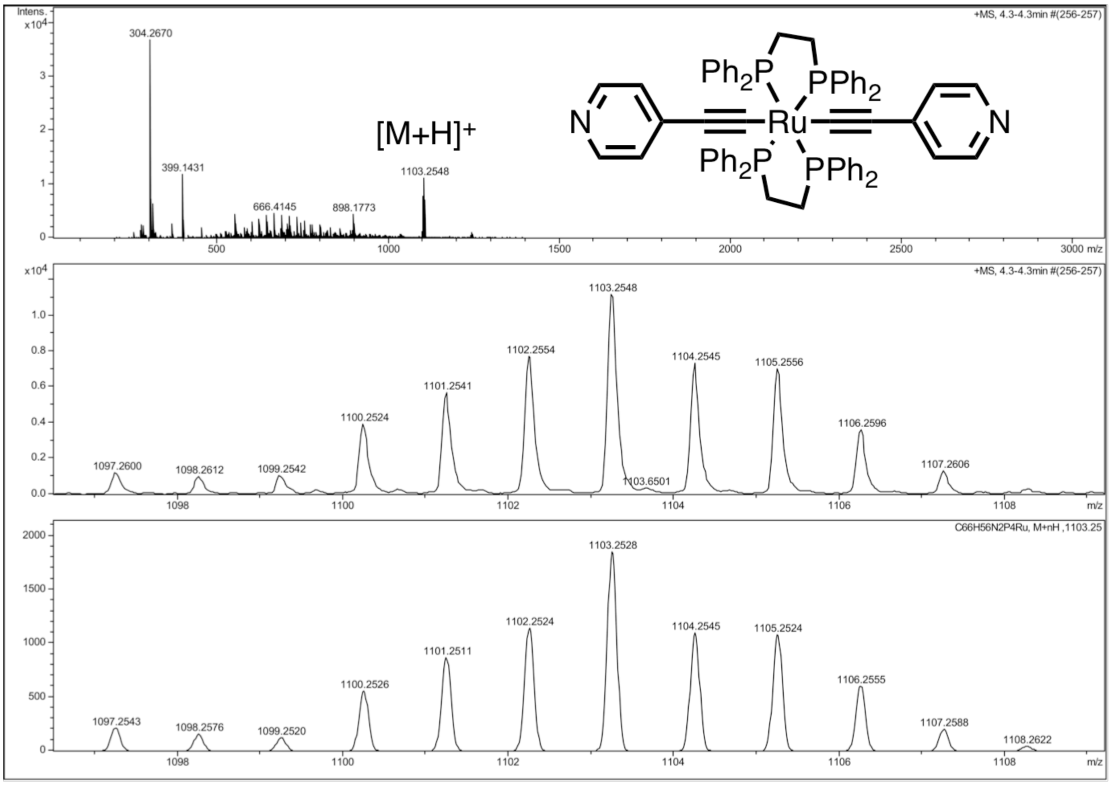

Figure S3f. ESI-TOF MS spectrum of **1**.

Synthesis of **2**

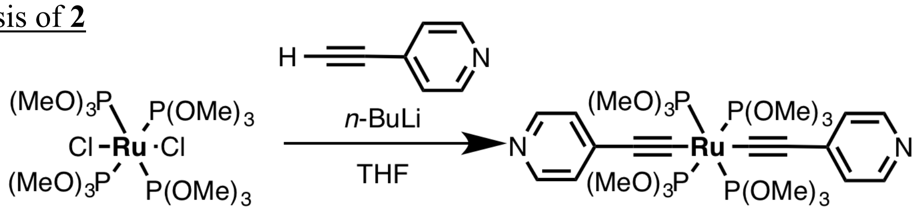

2

To a mixture of 4-ethynylpyridine (92.4 mg, 0.896 mmol) in THF (5 mL), cooled at –78 ºC was added *n*-BuLi (0.327 mL , 0.986 mmol) dropwise. After being stirred for 30 min at this temperature, a THF solution (10 mL) of Ru[P(OMe)$_3$]$_4$Cl$_2$ (150 mg, 0.224 mmol) was added via *cannula*. Then the mixture was refluxed for 15 min. The volatiles were removed in *vacuo*, and the products were extracted with CH_2Cl_2 and passed through a Celite® pad. The filtrate was concentrated to dryness and the residue was washed with diethyl ether, dissolved in ethanol, and precipitated with pentane. The filtrate was evaporated in *vacuo* to give a yellow solid (80.0 mg, 0.0998 mmol, 45%). The product is pure enough to be used for various measurements. The analytical pure sample was obtained by slow diffusion of methanol into CH_2Cl_2 solution of **1**.

^{1}H NMR (400 MHz, CD_2Cl_2, r.t.) : δ 8.24 (*pseudo*-d, 4H, J = 5.5 Hz, Py), 6.89 (*pseudo*-d, 4H, J = 5.5 Hz, Py), 3.85 (m, 36H, OCH_3). ^{31}P NMR (161 MHz, C_6D_6, r.t.) : δ 140 (s). ^{13}C NMR (126MHz, CD_2Cl_2, r.t.)**:** δ 149.4 (s, Py), 137.6 (s, Ru-C≡), 125.1 (s, Py), 113.8 (s, Ru-C≡C), 52.9 (s, OMe). Quaternary carbon atoms of pyridine could not be observed even in saturated CD_2Cl_2 solution. ESI-TOF MS (*m*/*z*): Calcd. for $C_{26}H_{45}N_2O_{12}P_4Ru$ 803.0969, Found. 803.0961 $[M+H]^+$. IR (KBr): 2073 cm^{-1}(C≡C). Anal. Calcd. For $C_{26}H_{44}N_2O_{12}P_4Ru \cdot CH_2Cl_2$: C, 36.58 ; H, 5.23 ; N, 3.16. Found : C, 36.42 ; H, 5.36 ; N, 3.43.

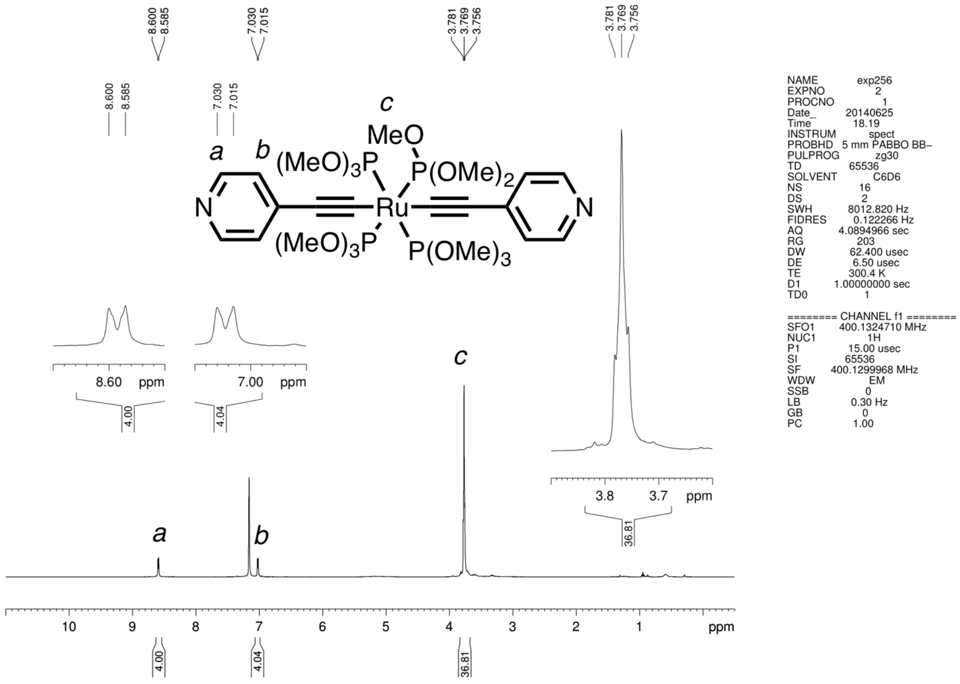

Figure S4a. ^{1}H NMR spectrum of **2** (400 MHz, CD_2Cl_2, r.t.)

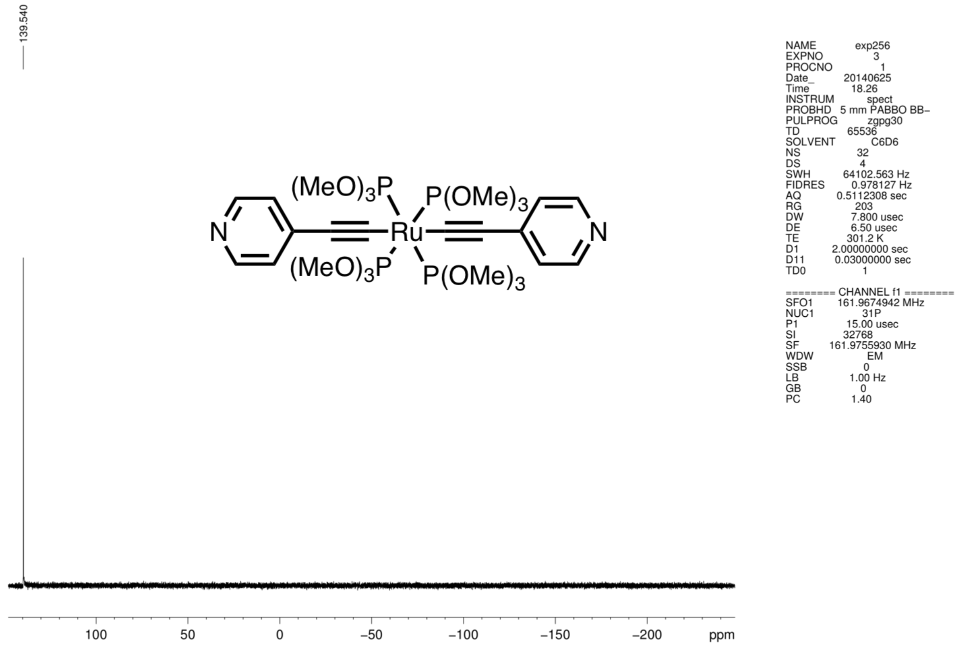

Figure S4b. ^{31}P NMR spectra of **2** (162 MHz, CD_2Cl_2, r.t.)

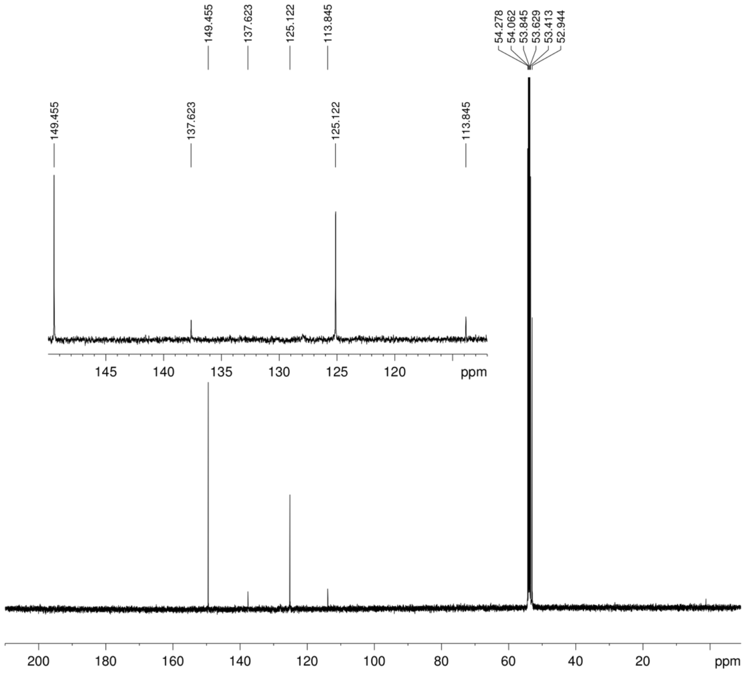

```
NAME     pyRu(P(OMe)3)4py
EXPNO              2
PROCNO             1
Date_        20140926
Time           17.02
INSTRUM          spect
PROBHD   5 mm CPPBBO BB
PULPROG          zgpg30
TD             65536
SOLVENT          CD2Cl2
NS               256
DS                 4
SWH          27573.529 Hz
FIDRES        0.420739 Hz
AQ           1.1884362 sec
RG              191.56
DW              18.133 usec
DE              18.00 usec
TE              291.9 K
D1          2.00000000 sec
D11         0.03000000 sec
TD0                1

======== CHANNEL f1 ========
SFO1       125.7703648 MHz
NUC1               13C
P1              10.00 usec
SI             32768
SF         125.7577406 MHz
WDW                EM
SSB                0
LB              1.00 Hz
GB                 0
PC              1.40
```

Figure S4c. ^{13}C NMR spectra of **2** (126 MHz, CD_2Cl_2, r.t.)

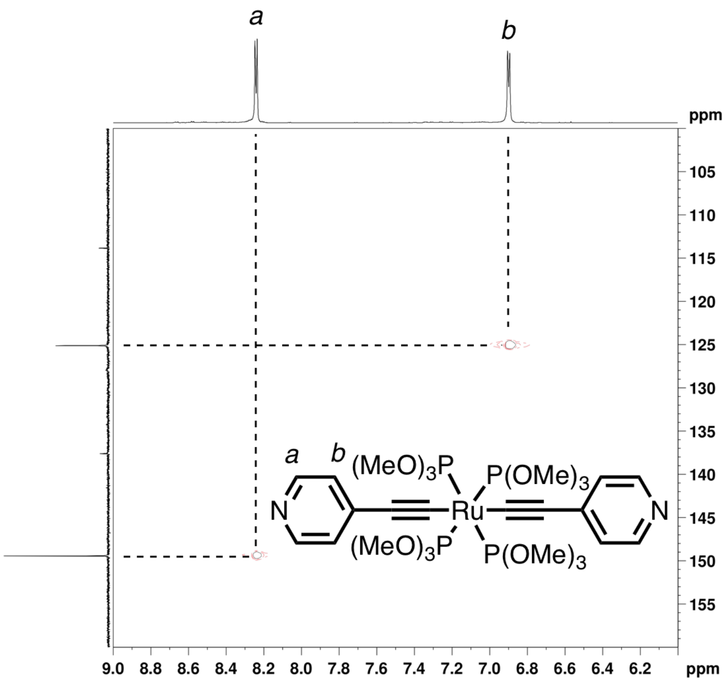

```
NAME     pyRu(P(OMe)3)4py
EXPNO              3
PROCNO             1
Date_        20140926
Time           20.05
INSTRUM          spect
PROBHD   5 mm CPPBBO BB
PULPROG     hsqcetgpsi2
TD              1024
SOLVENT          CD2Cl2
NS                 2
DS                16
SWH          6666.667 Hz
FIDRES        6.510417 Hz
AQ          0.0768500 sec
RG              191.56
DW              75.000 usec
DE              10.00 usec
TE              292.4 K
CNST2       145.0000000
D0          0.00000300 sec
D1          1.50000000 sec
D4          0.00172414 sec
D11         0.03000000 sec
D16         0.00020000 sec
D24         0.00086207 sec
IN0         0.00002400 sec
ZGOPTNS

======== CHANNEL f1 ========
SFO1       500.1330069 MHz
NUC1                1H
P1              12.00 usec
P2              24.00 usec
P28              0.00 usec
ND0                2
TD                76
SFO1         125.7672 MHz
FIDRES      274.122803 Hz
SW            165.650 ppm
FnMODE      Echo−Antiecho
SI              1024
SF         500.1300113 MHz
WDW              QSINE
SSB                2
LB               0.00 Hz
GB                 0
PC               1.40
SI              1024
MC2         echo−antiecho
SF         125.7577513 MHz
WDW              QSINE
SSB                2
LB               0.00 Hz
GB                 0
```

Figure S4d. A part of HSQC spectra of **2** (500 MHz, CD_2Cl_2, r.t.)

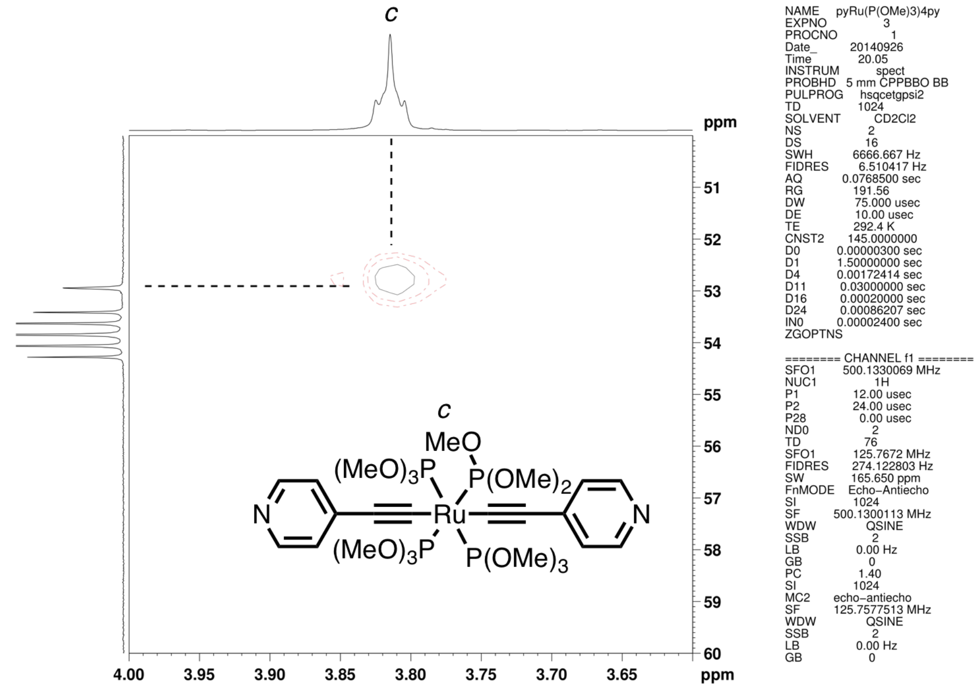

```
NAME     pyRu(P(OMe)3)4py
EXPNO              3
PROCNO             1
Date_         20140926
Time           20.05
INSTRUM          spect
PROBHD   5 mm CPPBBO BB
PULPROG     hsqcetgpsi2
TD             1024
SOLVENT          CD2Cl2
NS                 2
DS                16
SWH           6666.667 Hz
FIDRES         6.510417 Hz
AQ          0.0768500 sec
RG             191.56
DW             75.000 usec
DE             10.00 usec
TE             292.4 K
CNST2        145.0000000
D0         0.00000300 sec
D1         1.50000000 sec
D4         0.00172414 sec
D11         0.03000000 sec
D16         0.00020000 sec
D24         0.00086207 sec
IN0        0.00002400 sec
ZGOPTNS

======== CHANNEL f1 ========
SFO1        500.1330069 MHz
NUC1               1H
P1             12.00 usec
P2             24.00 usec
P28             0.00 usec
ND0                2
TD                76
SFO1         125.7672 MHz
FIDRES       274.122803 Hz
SW           165.650 ppm
FnMODE    Echo–Antiecho
SI            1024
SF         500.1300113 MHz
WDW              QSINE
SSB                2
LB              0.00 Hz
GB                 0
PC               1.40
SI            1024
MC2       echo–antiecho
SF         125.7577513 MHz
WDW              QSINE
SSB                2
LB              0.00 Hz
GB                 0
```

Figure S4e. A part of HSQC spectra of **2** (500 MHz, CD_2Cl_2, r.t.)

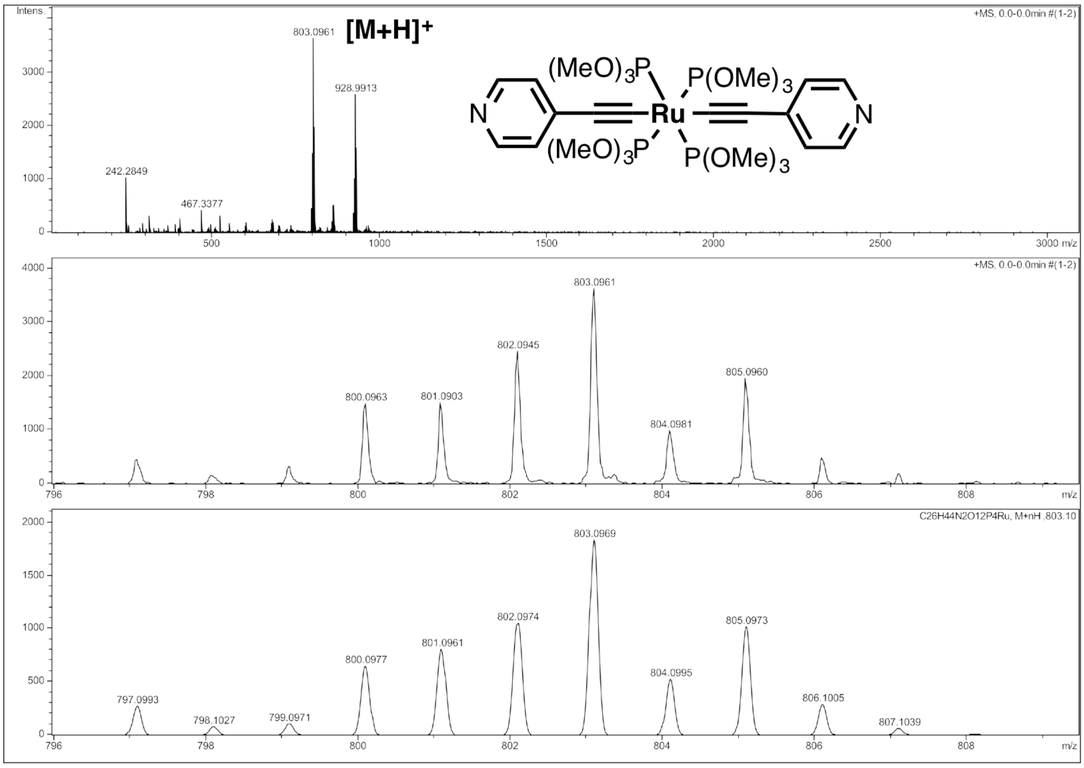

Figure S4f. ESI-TOF MS spectrum of **2**.

IV. Spectroscopy and Electrochemical Study

HOMO and LUMO of **1-3** were determined by the onset of the oxidation potential of cyclicvolatammograms and UV-Vis absorption spectra.

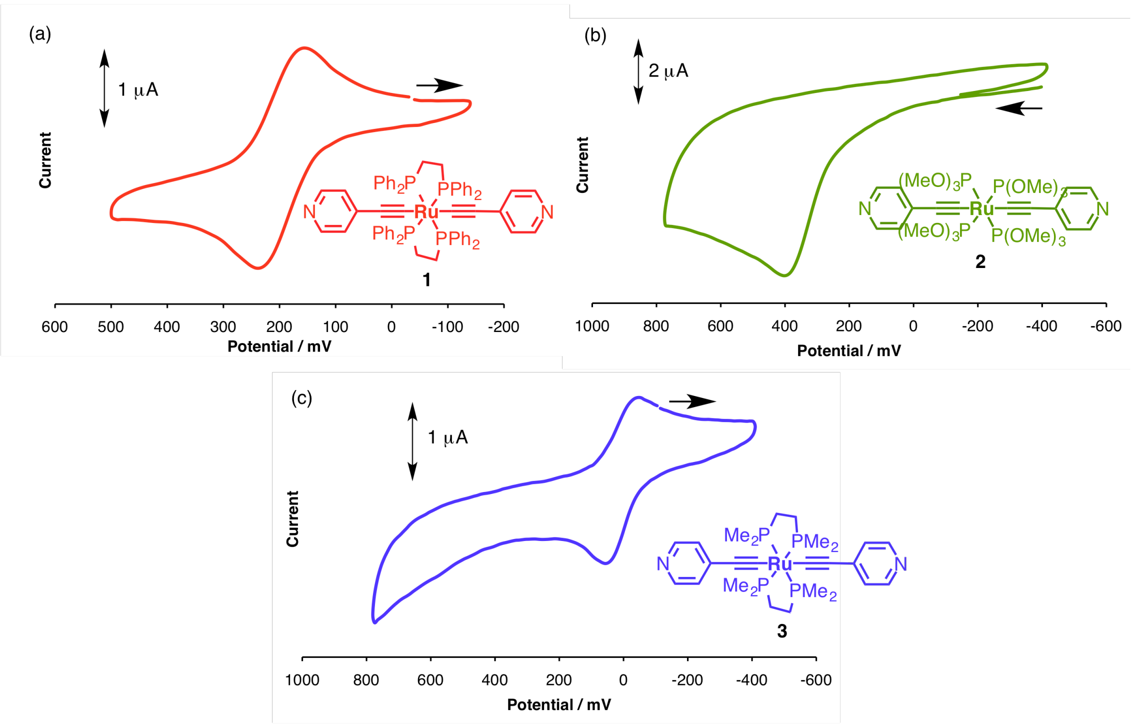

Figure S5. Cyclicvoltammograms of **1-3** in CH_2Cl_2.

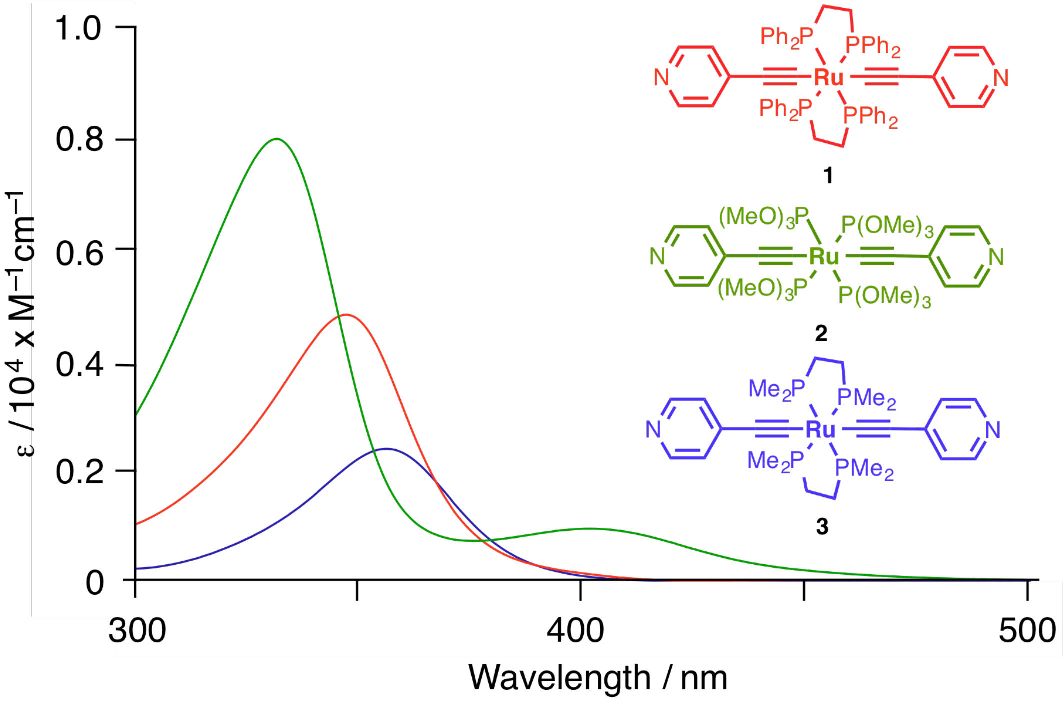

Figure S6. UV-Vis spectra of **1-3** in CH_2Cl_2.

IV. X-ray Diffraction Analysis

Method

Data collection and structural analysis of single crystals were performed on a Bruker Smart Apex II Ultra. All data were collected at –183 ℃. SHELXL crystallographic software package was used to solve the structure.

Table S1.

Identification code	Ru_pyridine	
Chemical formula	$C_{67}H_{58}Cl_2N_2P_4Ru$	
Formula weight	1187.01	
Temperature	90(2) K	
Wavelength	0.71073 Å	
Crystal system	triclinic	
Space group	P–1	
Unit cell dimensions	a = 10.5042(9) Å	α = 75.3940(10)°
	b = 12.4115(11) Å	β = 77.7320(10)°
	c = 22.3482(19) Å	γ = 86.4440(10)°
Volume	2754.9(4) $Å^3$	
Z	2	
Density (calculated)	1.431 g/cm^3	
Absorption coefficient	0.543 mm^{-1}	
F(000)	1224	
Theta range for data collection	1.70 to 25.02°	
Index ranges	-12<=h<=12, -14<=k<=14, -17<=l<=26	
Reflections collected	13071	
Independent reflections	9739 [R_{int} = 0.0137]	
Coverage of independent reflections	97.9%	
Absorption correction	multi-scan	
Refinement method	Full-matrix least-squares on F^2	
Refinement program	SHELXL-2013 (Sheldrick, 2013)	
Function minimized	$\Sigma\ w(F_o^2 - F_c^2)^2$	
Data / restraints / parameters	9739 / 0 / 685	
Goodness-of-fit on F2	0.929	
Δ / σ max	0.001	
Final R indices	7991 data;	
I>2 σ (I)	$R_1 = 0.0350, wR_2 = 0.1090$	
all data	$R_1 = 0.0458, wR_2 = 0.1195$	

Weighting scheme	$w=1/[\sigma^2(F_o^2)+(0.1000P)^2]$
where $P=(F_o^2+2F_c^2)/3$	
Largest diff. peak and hole	0.814 and -0.854 eÅ^{-3}
R.M.S. deviation from mean	0.074 eÅ^{-3}

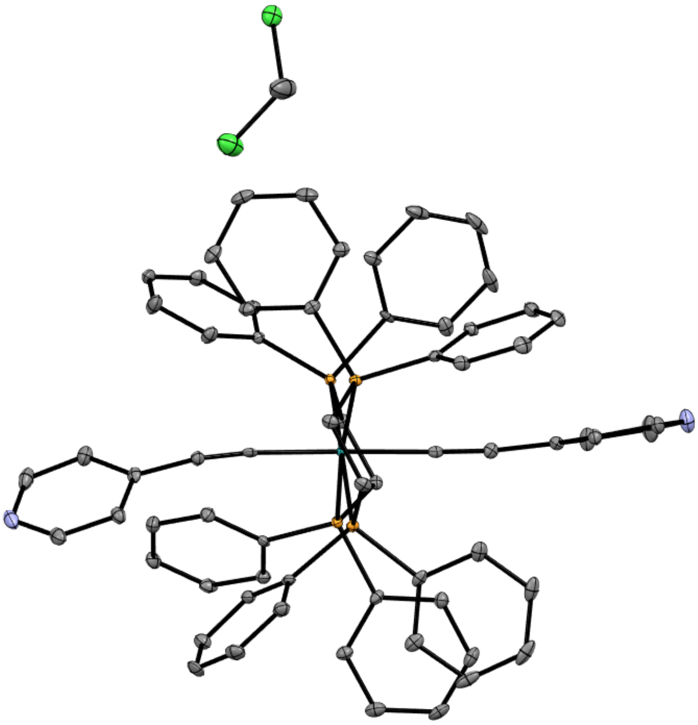

Figure S7. Ortep drawings of **1**•(CH_2Cl_2). Hydrogen atoms are omitted for clarity

V. DFT calculation

Computational conditions for molecular orbital calculations in the isolated condition

DFT calculations were performed by using the Gaussian 09 (D01) program package.[S7] Optimization of the geometries was carried out with the B3LYP/LanL2DZ (for Ru) and 6-31G* (for C, H, N, P) levels of theory and single point calculations were performed at the B3LYP/LanL2DZ (for Ru) and 6-311+G(d, p) (for C, H, N, P) levels of theory. The calculations were performed under vacuum conditions. No imaginary vibrational frequency was found in the vibrational frequency analysis for the optimized geometries.

As noted in the main text, LUMO to LUMO+2 of **1** are mainly localized on the dppe ligands, reflecting the electron accepting ability of dppe (Fig. S8 and S9). Because the ligand-localized orbitals should not be involved in conduction mechanism, we mainly discussed on LUMO+3 of **1** for comparison. For **2** and **3**, $P(OMe)_3$- and dmpe-based orbitals are observed in LUMO+2 and LUMO+3, respectively, though the energy levels of the orbitals are much higher than that of LUMO of **1**.

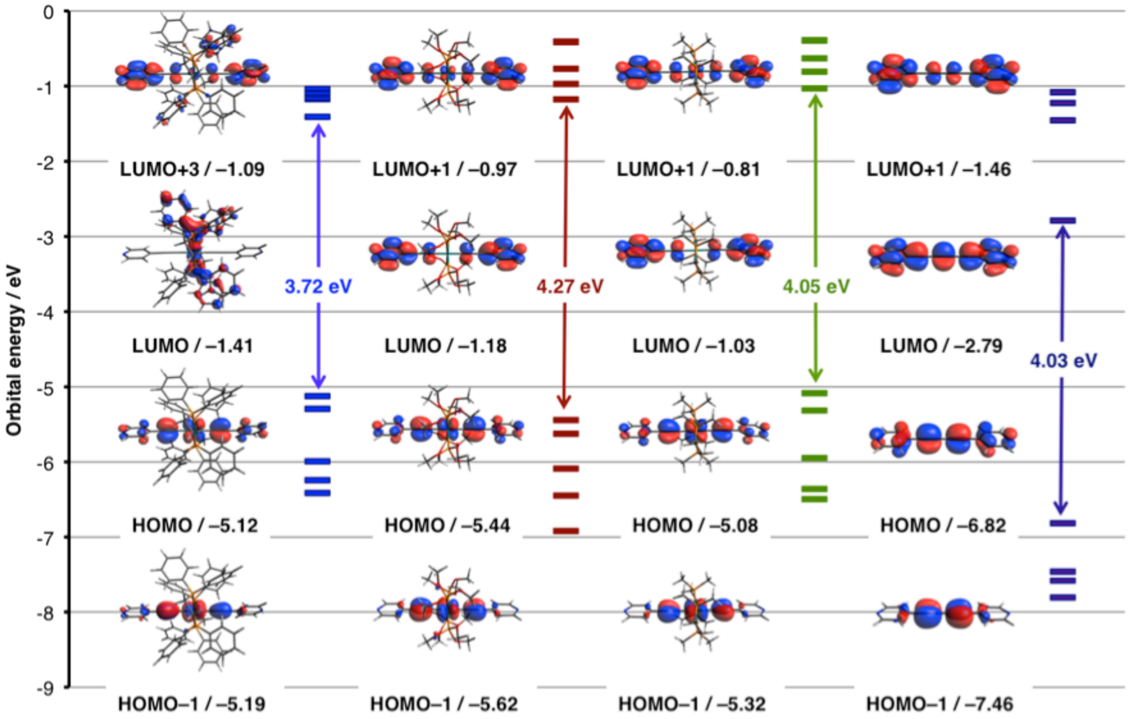

Figure S8. Kohn-Sham orbitals of **1**-**4** (from the left to the right).

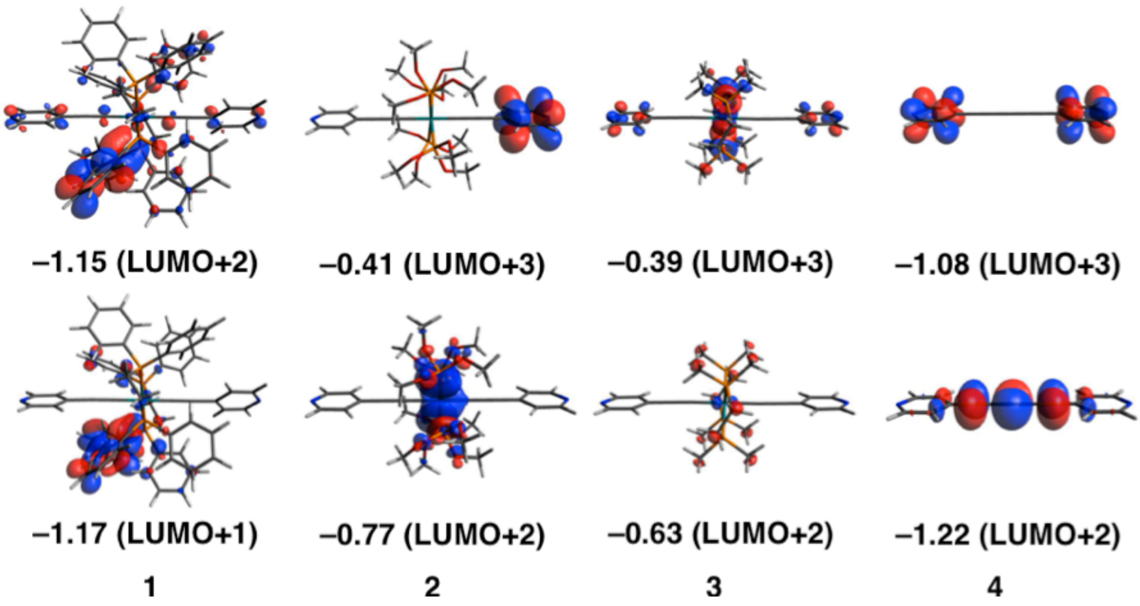

Figure S9. Selected Kohn-Sham orbitals of **1**-**4**.

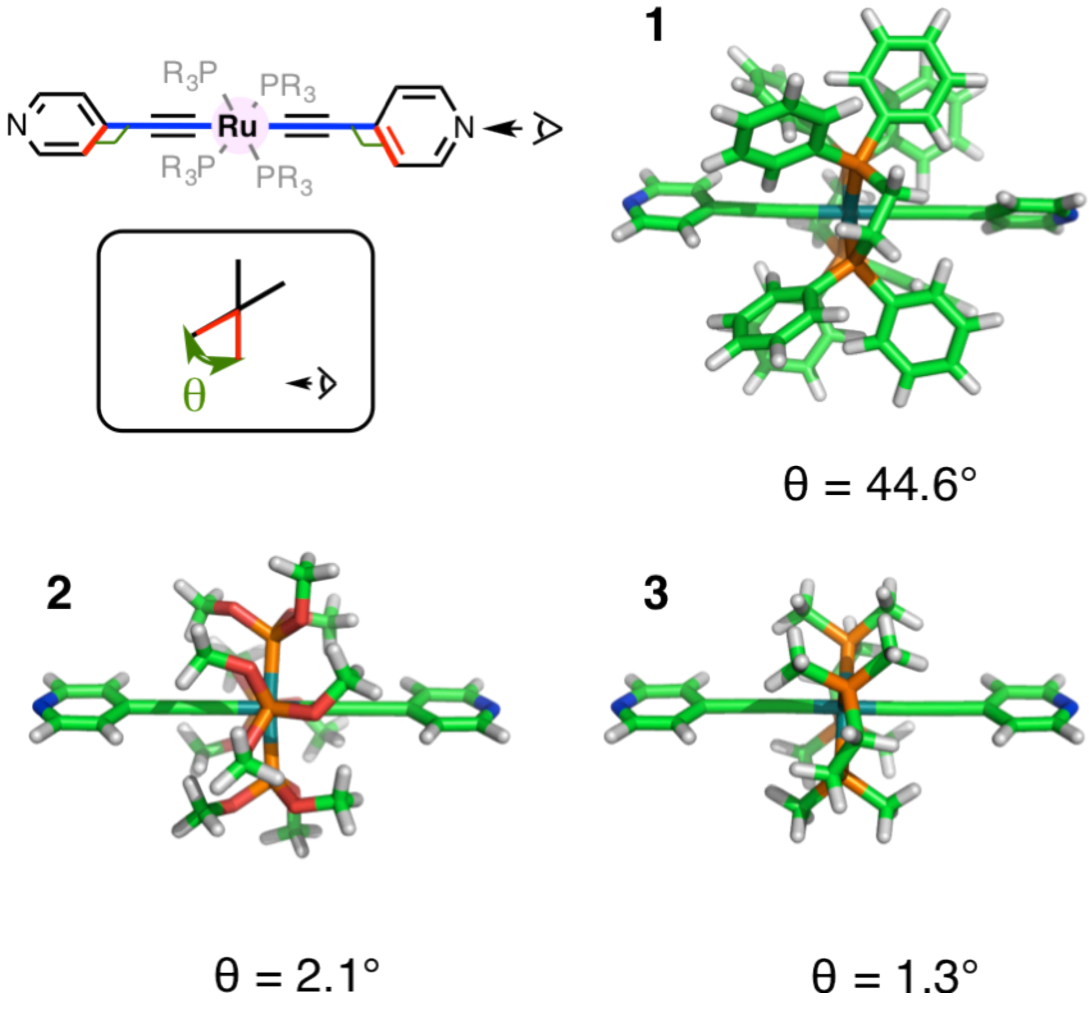

Figure S10. Computed dihedral angles of pyridine rings of **1-3.**

Computational conditions for electron transport calculations for Au-molecule-Au junction structures

DFT calculations for electron transport were performed by using the Gaussian 09 (D01) program package[S7] and the non-equilibrium Green's function (NEGF) method in a level-broadening approach.[S8] B3LYP/LanL2DZ (for Ru) and 6-31+G(d) (for C, H, N, P) levels of theory were adopted for the transport calculations. The computational procedure in the level-broadening approach is as follows.

I. Structural optimization of cluster models for Au-molecule-Au junctions.
II. Determination of the cluster sizes and scattering regions.
III. Calculations of transmission functions with the NEGF method.

In Step I (structural optimization), a small cluster model was adopted. Figure S11 shows a typical model in Step I, in which molecule **4** is sandwiched between Au_{20} clusters. The edge Au clusters inside the blue dotted lines in Fig. S11 are fixed to the bulk structure of Au metal. The assumption for the edge structure is reasonable because sandwiched molecules are connected to bulk electrodes in realistic situations. The structural relaxations were carried out for the rest atoms (e.g., Au_5-molcule **4**-Au_5 in Fig. S11). When target molecules to be sandwiched between electrodes are relatively small in size, the procedure in Step I can be executed in each case. Whereas target molecules are relatively large in size, we sometimes meet computational difficulities in structural relaxations, and the present target molecules corresponds to the difficult case. Since the target molecules (i.e., molecules **1**, **2**, **3**, and **4**) include pyridine rings at the molecular edges and the connections with electrodes are made by N-Au bonding, the structural information of Au_5-N in the relaxed Au_{20}-**4**-Au_{20} can be used for Au_{20}-**1**-Au_{20}, Au_{20}-**2**-Au_{20}, and Au_{20}-**3**-Au_{20}. In this way, we can construct reasonable Au_n-molecule-Au_n models even for large molecules. Note that the structural relaxation of molecules **1**, **2**, and **3** in the isolated conditions have to be done at first.

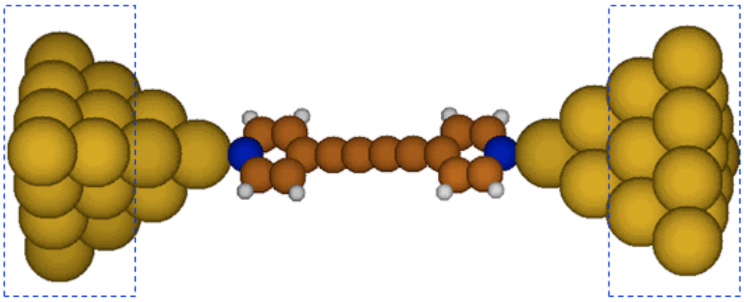

Figure S11. Cluster model of Au_{20}-**4**-Au_{20} for structural optimization.

Step II is related to the computational procedure in transmission calculations in Step III, and thus we firstly introduce the essence of the NEGF method with the broadening approach.

1) The cluster model for a molecular junction is composed of a left metal cluster, a sandwiched molecule and a right metal cluster, as shown in Fig. S12(a).

2) The sandwiched molecule and some metal atoms in both clusters are defined as an extended molecule (EM in Fig. S12(a)).

3) Metal cluster atoms except for the metal atoms in the EM region are recognized as electrode clusters, and the density of states of the metal clusters are broadened (i.e., level-broadening) to obtain Green's functions of the metal clusters.

4) Broadening parameters for the metal clusters are chosen so as to show a reasonable conductance in a reference system (e.g., $2e^2/h$ in a one-dimensional gold chain).

5) The size of the metal cluster and EM region are determined to hold the condition that the calculated conductance is almost insensitive to those sizes.

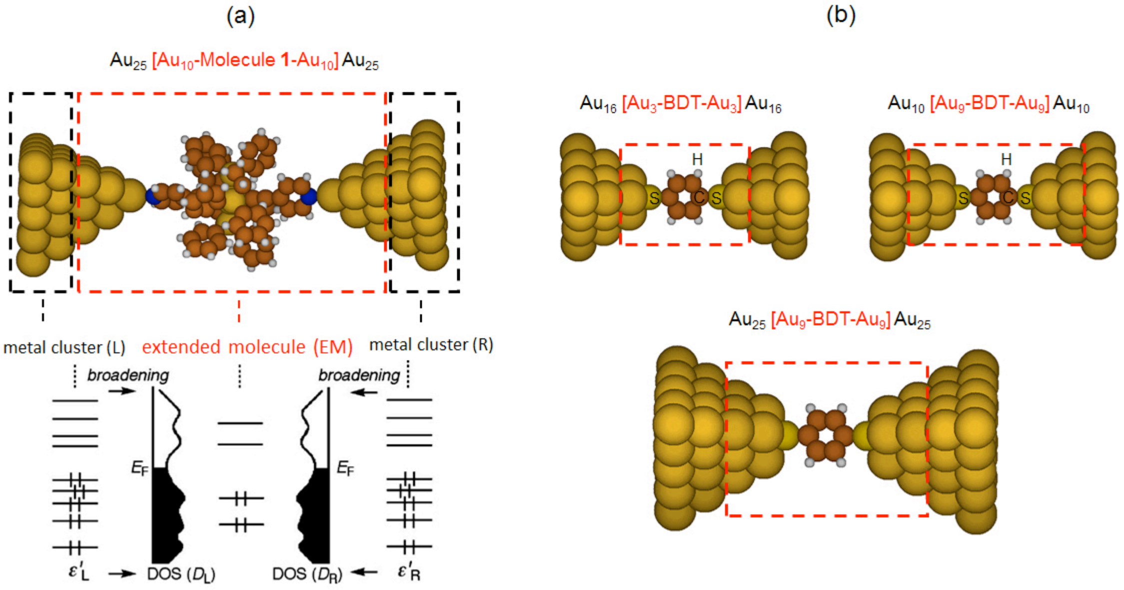

Figure S12. (a) Model definition in a level-broadening approch. (b) Cluster models for benzene-dithiole molecular junctions.

Figure S12(b) shows computational models for benzene dithiole (BDT) molecular junctions. The BDT junction is a benchmark junction, and the model is convenient to determine the appropriate size for clusters and EM region. In the notation of Au$_n$[Au$_m$-molecule-Au$_m$]Au$_n$ in Fig. S11, Au$_n$ corresponds to the metal cluster in the left/right side, and [Au$_m$-molecule-Au$_m$] is the extended molecule. As for the level-broadening for Au clusters, we adopted the broadening parameter of 1.0 eV for Au which was already determined in a separate calculation for the one-dimensional gold chain.[S8] The calculated conductance of BDT junctions together with the experimental value is listed in Table S1. The order of the calculated conductance is 10^{-2} G_0 showing a good correspondence to the experimental value. In the four models of the BDT junctions, EM of [Au_9-BDT-Au_9] is better than [Au_3-BDT-Au_3]. Thus we adopted Au_9 for metal in EM in the left/right side and Au_{25} for metal electrodes. Note that the target molecular junction in this study is a kind of the on-top connection with Au-N, and thus the cluster model must be Au_{25}[Au_{10}-molecule-Au_{10}]Au_{25} (See Fig. S12(a)). Now that the cluster size and EM region are determined, we can construct cluster models for transmission calculations as Au_{25}[Au_{10}-**1**-Au_{10}]Au_{25}, Au_{25}[Au_{10}-**2**-Au_{10}]Au_{25}, Au_{25}[Au_{10}-**3**-Au_{10}]Au_{25}, and Au_{25}[Au_{10}-**4**-Au_{10}]Au_{25}. The inset of Figure 12(a) corresponds to Au_{25}[Au_{10}-**1**-Au_{10}]Au_{25} and Au_{25}[Au_{10}-**4**-Au_{10}]Au_{25}.

Table S1: Calculated and experimental conductance of BDT junctions.

Method	**Model**	**Conductance/G_0**
NEGF-B3LYP/Lanl2DZ	Au_{16}[Au_3-BDT-Au_3]Au_{16}	**0.022**
	Au_{31}[Au_3-BDT-Au_3]Au_{31}	**0.022**
	Au_{10}[Au_9-BDT-Au_9]Au_{10}	**0.018**
	Au_{25}[Au_9-BDT-Au_9]Au_{25}	**0.017**
Experiment	—	**0.011**[a]

[a] Ref. S9

Table S2. Atomic Coordinates of **1.**

Ru	-0.03355	0.01294	0.00718	C	-2.70319	1.87436	2.38939
P	-0.09552	-1.55438	-1.85349	H	-2.84428	1.23147	1.52979
P	0.52719	1.64182	-1.72680	C	-3.63274	3.15876	4.22202
C	-2.02317	0.29924	-0.46886	H	-4.49059	3.50809	4.78522
C	1.98043	-0.26926	0.38913	C	1.23124	3.07272	1.78737
C	1.56203	5.47143	1.64001	C	3.47158	3.99771	1.76510
H	1.14561	6.46997	1.56947	H	4.54429	3.84471	1.77522
C	-4.54357	0.74195	-1.17922	C	2.94539	5.28893	1.68984
C	3.18269	-0.42360	0.63081	H	3.60855	6.14591	1.66032
C	-4.88170	1.58346	-2.26462	C	2.62061	2.89236	1.80603
H	-4.09602	2.06195	-2.83516	H	3.03553	1.89360	1.81392
C	-3.19210	0.49092	-0.82137	C	0.70636	4.36854	1.68774
C	-5.62035	0.16763	-0.46310	H	-0.36556	4.52010	1.66312
H	-5.41631	-0.48173	0.37916	C	-1.37991	-2.92131	-2.03255
C	4.57159	-0.61215	0.85306	C	-3.66154	-3.62392	-2.46578
C	5.41742	-1.15646	-0.14342	H	-4.68738	-3.36821	-2.70618
H	4.99678	-1.45881	-1.09348	C	-2.71288	-2.60676	-2.33490
N	-7.25030	1.24646	-1.89173	H	-3.01953	-1.57507	-2.44109
N	7.36204	-0.98041	1.28993	C	-1.96600	-5.27431	-1.98455
C	5.18832	-0.26703	2.07905	H	-1.66954	-6.30859	-1.85130
H	4.59384	0.15199	2.88216	C	-3.29146	-4.95913	-2.28932
C	-6.92656	0.44536	-0.85019	H	-4.02898	-5.74682	-2.39173
H	-7.75760	0.00895	-0.30457	C	-1.01162	-4.26150	-1.86193
C	6.77310	-1.31613	0.11788	H	0.01742	-4.51475	-1.63991
H	7.42525	-1.73373	-0.64304	C	1.46065	-2.46646	-2.38923
C	-6.21994	1.79829	-2.57418	C	2.93815	-3.35098	-4.10069
H	-6.48633	2.44316	-3.40577	H	3.18872	-3.47136	-5.14855
C	6.55481	-0.46408	2.24457	C	3.74948	-3.91857	-3.11528
H	7.03049	-0.19792	3.18343	H	4.63319	-4.47999	-3.39623
C	-1.41270	2.26401	2.76073	C	3.41514	-3.76266	-1.76858
C	-3.80994	2.32564	3.11821	H	4.03477	-4.19855	-0.99399
H	-4.80523	2.02232	2.81430	C	2.28075	-3.03119	-1.40386
C	-2.34261	3.54361	4.60226	H	2.04636	-2.89238	-0.35797
H	-2.19839	4.18957	5.46099	C	1.79422	-2.63573	-3.73981
C	-1.23789	3.09839	3.87720	H	1.16413	-2.22406	-4.51823
H	-0.24208	3.41171	4.16892	C	-2.16662	-2.31435	2.18013

C	-4.35418	-3.05542	1.44455
H	-5.07126	-3.18539	0.64224
C	-4.65984	-3.47215	2.74042
H	-5.62292	-3.92017	2.95688
C	-2.47119	-2.75061	3.47843
H	-1.73863	-2.66240	4.27175
C	-3.11435	-2.47042	1.16476
H	-2.89394	-2.13810	0.16174
C	-3.71464	-3.31834	3.75858
H	-3.94099	-3.64786	4.76623
C	-0.62412	3.09520	-2.05881
C	-0.53399	3.82138	-3.25562
H	0.21915	3.56708	-3.99265
C	-1.57686	3.46631	-1.10561
H	-1.66677	2.89908	-0.19052
C	-1.39146	4.89596	-3.49680
H	-1.31186	5.45063	-4.42480
C	-2.34666	5.25699	-2.54236
H	-3.01584	6.08850	-2.73128
C	-2.43530	4.54310	-1.34652
H	-3.17781	4.81074	-0.60375
C	4.78014	3.56808	-2.08091
H	5.76952	4.00217	-2.16953
C	2.22304	2.44533	-1.85495
C	4.61763	2.18097	-2.12672
H	5.47962	1.53275	-2.23292
C	3.34531	1.62038	-2.01352
H	3.23094	0.54367	-2.01730
C	2.39015	3.83152	-1.79292
H	1.53211	4.47493	-1.65062
C	0.57671	-3.14694	1.90924
C	0.02932	-4.38882	1.56278
H	-1.00706	-4.45678	1.25673
C	0.81586	-5.54239	1.61520
H	0.38205	-6.49913	1.34708
C	1.91694	-3.07340	2.31103
H	2.36161	-2.11710	2.54860
C	2.69902	-4.22981	2.36767
H	3.73492	-4.15898	2.67908
C	2.15065	-5.46645	2.01875
H	2.75811	-6.36312	2.06290
C	-0.50596	-0.45080	-3.35644
H	-0.50626	-1.03960	-4.27745
H	-1.51449	-0.07091	-3.17652
C	0.49640	0.70354	-3.41095
H	0.23933	1.41034	-4.20381
H	1.51114	0.33539	-3.58658
P	-0.47276	-1.58482	1.79431
P	0.09427	1.58070	1.85296
C	0.81938	0.53077	3.28154
H	1.83004	0.24938	2.98451
H	0.84638	1.13614	4.19239
C	-0.07532	-0.70037	3.46950
H	-1.04196	-0.39981	3.88434
H	0.39110	-1.42888	4.13905
C	3.66567	4.39001	-1.90986
H	3.78422	5.46629	-1.85994

Table S3. Atomic Coordinates of **2**.

Ru	-0.00272	-0.00002	0.00001
P	0.12235	-1.01301	-2.14667
P	0.12257	1.01283	2.14672
P	-0.12231	2.14507	-1.01317
P	-0.12231	-2.14502	1.01331
O	0.94151	-0.05420	-3.17687
O	-1.21323	-1.26584	-3.04833
O	0.81047	-2.48212	-2.37823
O	-1.21295	1.26581	3.04843
O	0.94160	0.05381	3.17682
O	0.81094	2.48182	2.37834
O	-0.81303	2.37663	-2.48099
O	1.21792	3.03916	-1.27278
O	-0.93278	3.18383	-0.05455
O	-0.81279	-2.37640	2.48128
O	1.21792	-3.03916	1.27281
O	-0.93301	-3.18380	0.05490
C	-2.08840	0.00001	0.00010
C	-3.31989	0.00002	0.00005
C	-4.74227	0.00008	-0.00007
C	-5.49209	-1.19607	-0.03177
C	-6.88219	-1.13732	-0.03041
N	-7.59202	0.00018	-0.00026
C	-6.88211	1.13762	0.02999
C	-5.49201	1.19627	0.03154
C	2.08341	-0.00006	-0.00007
C	3.31474	-0.00003	-0.00011
C	4.73771	0.00004	-0.00021
C	5.48734	-1.19641	0.01101
C	6.87745	-1.13768	0.00944
N	7.58729	0.00016	-0.00041
C	6.87735	1.13794	-0.01017
C	5.48723	1.19655	-0.01154
C	1.00648	-0.33821	-4.58502
C	-2.19229	-2.27054	-2.73256
C	2.17336	-2.76189	-2.01317
C	-2.19186	2.27069	2.73276
C	1.00667	0.33773	4.58500
C	2.17387	2.76136	2.01323
C	2.18540	2.72343	-2.28899
C	-0.98849	4.59112	-0.34321
C	-2.17406	-2.00619	2.76357
C	2.18553	-2.72334	2.28887
C	-0.98877	-4.59107	0.34367
H	-4.98325	-2.15509	-0.05820
H	-7.46292	-2.05920	-0.05527
H	-7.46278	2.05954	0.05478
H	-4.98309	2.15525	0.05804
H	4.97872	-2.15566	0.02198
H	7.45815	-2.05990	0.01716
H	7.45797	2.06021	-0.01796
H	4.97852	2.15575	-0.02244
H	-2.97080	-2.17658	-3.49308
H	-2.61318	-2.09391	-1.74171
H	-1.74116	-3.26503	-2.78457
H	1.82237	0.26983	-4.98158
H	0.06579	-0.06205	-5.06775
H	1.21381	-1.39697	-4.76467
H	2.41096	-3.72694	-2.46790
H	2.27820	-2.82217	-0.92923
H	2.84745	-1.99391	-2.40298
H	2.95909	3.49100	-2.21122
H	1.72105	2.76687	-3.27764
H	2.61589	1.73645	-2.11369
H	1.82246	-0.27049	4.98149
H	0.06595	0.06170	5.06774
H	1.21419	1.39643	4.76471
H	2.95919	-3.49096	2.21110
H	2.61603	-1.73639	2.11340
H	1.72129	-2.76665	3.27758
H	-1.79573	-4.99711	-0.27017
H	-1.20380	-4.76861	1.40133

H	-0.04216	-5.06786	0.07749
H	-2.39979	-2.42975	3.74532
H	-2.85397	-2.42512	2.01626
H	-2.28566	-0.92194	2.78917
H	-2.97037	2.17682	3.49328
H	-2.61279	2.09418	1.74190
H	-1.74057	3.26510	2.78482
C	-2.17440	2.00663	-2.76307
H	-2.40024	2.43028	-3.74476
H	-2.85413	2.42561	-2.01562
H	-2.28616	0.92240	-2.78872
H	2.41162	3.72639	2.46794
H	2.27869	2.82160	0.92929
H	2.84784	1.99328	2.40305
H	-1.79533	4.99718	0.27079
H	-1.20368	4.76875	-1.40082
H	-0.04181	5.06783	-0.07714

Table S4. Atomic Coordinates of **3.**

Ru	0.00000	0.00007	0.00002
P	-0.13081	-1.76601	1.58539
P	0.13060	-1.76543	-1.58602
C	-2.07961	0.00014	-0.07465
C	2.07961	-0.00002	0.07468
C	-4.73721	0.00003	-0.08362
C	3.31486	-0.00011	0.07984
C	-5.48862	-1.19616	-0.08279
H	-4.97997	-2.15574	-0.08237
C	-3.31486	0.00012	-0.07982
C	-5.48880	1.19610	-0.08367
H	-4.98031	2.15576	-0.08395
C	4.73721	-0.00018	0.08360
C	5.48866	-1.19633	0.08335
H	4.98006	-2.15593	0.08342
N	-7.58930	-0.00019	-0.08086
N	7.58930	-0.00028	0.08076
C	5.48876	1.19592	0.08304
H	4.98022	2.15556	0.08284
C	-6.87858	1.13741	-0.08224
H	-7.45886	2.06003	-0.08180
C	6.87845	-1.13780	0.08191
H	7.45863	-2.06049	0.08122
C	-6.87840	-1.13769	-0.08141
H	-7.45856	-2.06039	-0.08029
C	6.87854	1.13729	0.08159
H	7.45879	2.05993	0.08068
C	-1.36246	2.14429	-2.60967
C	1.49217	1.85287	-2.83366
C	-1.49211	-1.85282	2.83375
C	1.36251	-2.14422	2.60965
C	-1.49219	1.85232	2.83410
C	-1.36260	-2.14267	-2.61079
C	1.49219	-1.85216	-2.83406
C	1.36260	2.14283	2.61075
C	-0.40681	-3.36021	0.64845
H	-1.48017	-3.40881	0.42660
C	0.40585	-3.36014	-0.64967
H	0.16046	-4.22298	-1.28133
H	1.47919	-3.40936	-0.42784
P	-0.13063	1.76557	1.58603
P	0.13082	1.76610	-1.58536
C	0.40677	3.36033	-0.64845
H	1.48011	3.40898	-0.42658
H	0.16175	4.22353	-1.27978
C	-0.40592	3.36026	0.64966
H	-1.47925	3.40945	0.42782
H	-0.16054	4.22312	1.28132
H	-1.56599	2.85645	3.26683
H	-1.31082	1.13953	3.64388
H	-2.43265	-1.58778	2.34357
H	-1.31034	-1.14035	3.64373
H	1.53114	1.32632	3.32017
H	1.24756	3.07972	3.16758
H	2.24020	2.19298	1.96147
H	-2.24021	-2.19298	-1.96153
H	-1.24747	-3.07949	-3.16774
H	-1.53119	-1.32608	-3.32011
H	1.31079	-1.13941	-3.64387
H	1.56606	-2.85629	-3.26676
H	2.43267	-1.58746	-2.34356
H	-1.56607	-2.85706	3.26617
H	2.23994	-2.19456	1.96016
H	1.24717	-3.08126	3.16619
H	1.53160	-1.32804	3.31931
H	-1.53148	1.32815	-3.31940
H	-1.24715	3.08137	-3.16615
H	-2.23993	2.19454	-1.96021
H	1.56620	2.85711	-3.26608
H	1.31042	1.14040	-3.64365
H	2.43269	1.58781	-2.34342
H	-0.16182	-4.22343	1.27976

H	-2.43269	1.58770	2.34360

Table S5. Atomic coordinates of **4.**

Ru	0.00000	0.00007	0.00002	H	-1.48017	-3.40881	0.42660
P	-0.13081	-1.76601	1.58539	C	0.40585	-3.36014	-0.64967
P	0.13060	-1.76543	-1.58602	H	0.16046	-4.22298	-1.28133
C	-2.07961	0.00014	-0.07465	H	1.47919	-3.40936	-0.42784
C	2.07961	-0.00002	0.07468	P	-0.13063	1.76557	1.58603
C	-4.73721	0.00003	-0.08362	P	0.13082	1.76610	-1.58536
C	3.31486	-0.00011	0.07984	C	0.40677	3.36033	-0.64845
C	-5.48862	-1.19616	-0.08279	H	1.48011	3.40898	-0.42658
H	-4.97997	-2.15574	-0.08237	H	0.16175	4.22353	-1.27978
C	-3.31486	0.00012	-0.07982	C	-0.40592	3.36026	0.64966
C	-5.48880	1.19610	-0.08367	H	-1.47925	3.40945	0.42782
H	-4.98031	2.15576	-0.08395	H	-0.16054	4.22312	1.28132
C	4.73721	-0.00018	0.08360	H	-1.56599	2.85645	3.26683
C	5.48866	-1.19633	0.08335	H	-1.31082	1.13953	3.64388
H	4.98006	-2.15593	0.08342	H	-2.43265	-1.58778	2.34357
N	-7.58930	-0.00019	-0.08086	H	-1.31034	-1.14035	3.64373
N	7.58930	-0.00028	0.08076	H	1.53114	1.32632	3.32017
C	5.48876	1.19592	0.08304	H	1.24756	3.07972	3.16758
H	4.98022	2.15556	0.08284	H	2.24020	2.19298	1.96147
C	-6.87858	1.13741	-0.08224	H	-2.24021	-2.19298	-1.96153
H	-7.45886	2.06003	-0.08180	H	-1.24747	-3.07949	-3.16774
C	6.87845	-1.13780	0.08191	H	-1.53119	-1.32608	-3.32011
H	7.45863	-2.06049	0.08122	H	1.31079	-1.13941	-3.64387
C	-6.87840	-1.13769	-0.08141	H	1.56606	-2.85629	-3.26676
H	-7.45856	-2.06039	-0.08029	H	2.43267	-1.58746	-2.34356
C	6.87854	1.13729	0.08159	H	-1.56607	-2.85706	3.26617
H	7.45879	2.05993	0.08068	H	2.23994	-2.19456	1.96016
C	-1.36246	2.14429	-2.60967	H	1.24717	-3.08126	3.16619
C	1.49217	1.85287	-2.83366	H	1.53160	-1.32804	3.31931
C	-1.49211	-1.85282	2.83375	H	-1.53148	1.32815	-3.31940
C	1.36251	-2.14422	2.60965	H	-1.24715	3.08137	-3.16615
C	-1.49219	1.85232	2.83410	H	-2.23993	2.19454	-1.96021
C	-1.36260	-2.14267	-2.61079	H	1.56620	2.85711	-3.26608
C	1.49219	-1.85216	-2.83406	H	1.31042	1.14040	-3.64365
C	1.36260	2.14283	2.61075	H	2.43269	1.58781	-2.34342
C	-0.40681	-3.36021	0.64845	H	-0.16182	-4.22343	1.27976

H	-2.43269	1.58770	2.34360

VII. References

[S1] B. Mühling, S. Theisinger, and H. Meier, *Synthesis*, 2006, **6**, 1009.

[S2] M. A. Fox, J. E. Harris, S. Heider, V. Pérez-Gregorio, M. E. Zakrzewska, J. D. Farmer, D. S. Yufit, J. A.K. Howard, and P. J. Low *J. Organometallic Chem.*, 2009, **694**, 2350.

[S3] T. Cardolaccia, A. M. Funston, M. E. Kose , J. M. Keller , J. R. Miller, and K. S. Schanze, *J. Phys. Chem. B*, 2007, **111**, 10871.

[S4] G. Albertin , S. Autoniutti , E. Bordignon , F. Cazzaro , S. Ianelli , and G. Pelizzi, *Organometallics*, 1995, **14**, 4114.

[S5] D. Xu, W. Zhu, Q. An, W. Li, X. Li, H. Yang, J. Yina and G. Li, *Chem. Commun.*, 2012, **48**, 3494.

[S6] F. E. Kühn, J.-L. Zuo, F. F. de Biani, A. M. Santos, Y. Zhang, J. Zhao, A. Sandulache and E. Herdtweck, *New J. Chem.*, 2004, **28**, 43.

[S7] Gaussian 09, Revision D.01, M. J. Frisch, G. W. Trucks, H. B. Schlegel, G. E. Scuseria, M. A. Robb, J. R. Cheeseman, G. Scalmani, V. Barone, B. Mennucci, G. A. Petersson, H. Nakatsuji, M. Caricato, X. Li, H. P. Hratchian, A. F. Izmaylov, J. Bloino, G. Zheng, J. L. Sonnenberg, M. Hada, M. Ehara, K. Toyota, R. Fukuda, J. Hasegawa, M. Ishida, T. Nakajima, Y. Honda, O. Kitao, H. Nakai, T. Vreven, J. A. Montgomery, J. E. Peralta Jr., F. Ogliaro, M. Bearpark, J. J. Heyd, E. Brothers, K. N. Kudin, V. N. Staroverov, R. Kobayashi, J. Normand, K. Raghavachari, A. Rendell, J. C. Burant, S. S. Iyengar, J. Tomasi, M. Cossi, N. Rega, J. M. Millam, M. Klene, J. E. Knox, J. B. Cross, V. Bakken, C. Adamo, J. Jaramillo, R. Gomperts, R. E. Stratmann, O. Yazyev, A. J. Austin, R. Cammi, C. Pomelli, J. W. Ochterski, R. L. Martin, K. Morokuma, V. G. Zakrzewski, G. A. Voth, P. Salvador, J. J. Dannenberg, S. Dapprich, A. D. Daniels, Ö Farkas, J. B. Foresman, J. V. Ortiz, J. Cioslowski, and D. J. Fox. Gaussian, Inc., Wallingford CT, 2009.

[S8] T. Tada, M. Kondo and K. Yoshizawa, *J. Chem. Phys.*, 2004, **121**, 8050.

[S9] X. Xiao, B. Xu and N. J. Tao, *Nano Lett.*, 2004, **4**, 267